

Non-Dissipative Logic Device NOT Based on Two Coupled Quantum Dots

L.A.Openov and A.M.Bychkov

*Moscow State Engineering Physics Institute (Technical University),
Moscow, 115409, Russia*

Non-dissipative dynamics of interacting electrons in two tunnel-coupled quantum dots is studied theoretically within the framework of the Hubbard model. Various values of intra-dot Coulomb repulsion energy U and inter-dot tunneling energy V are considered, which correspond to various size of the dots and to various distance between them. In the ground state, the average value of the spin projection (magnetic moment) at each dot is zero. The input signal (the local external magnetic field H) applied to one of the dots at a time $t = 0$ causes the electronic subsystem to evolve in such a way that magnetic moments of quantum dots become oriented in the opposite directions at any time $t > 0$. For any set of U and V , there exist optimal values of H and t which maximize the absolute values of magnetic moments at both dots, and magnetic moments become almost saturated. Thus, the antiferromagnetic-like spin ordering can be realized at the stage of coherent temporal evolution, well before the relaxation to a new ground state at the sacrifice of inelastic processes. This effect ("dynamical antiferromagnetism") may be used for implementation of a logic function NOT in an extremely short time. A possibility to use the arrays of quantum dots as high-speed single-electron devices of new generation is discussed.

1. Introduction

Feynman's original idea [1] to use the states of a quantum mechanical system for information coding and processing has stimulated the work on a quantum theory of computation [2]. This theory takes advantage of fundamental properties of quantum systems, such as superposition, interference, entanglement, nonlocality, and uncertainty. The quantum bit ("qubit") can exist in arbitrary superpositions of classical bits, 0 and 1. In this way it appears to be possible to develop very efficient computational algorithms which are exponentially faster than conventional ones [3]. The first experimental demonstrations of quantum gates (elementary units capable to perform simplest logical operations) have been reported recently [4,5]. They are based on encoding the qubits in photon states. However, a lot of skepticism has been given to a possibility of practical utilization of such gates in a quantum computer [6,7].

Another way is to use quantum mechanical systems to employ *classical* Boolean logic. For example, Lent *et al.* [8] have proposed to represent the bits 0 and 1 by two opposite charge polarizations of a cell containing five quantum dots occupied by two electrons. Proper lateral arrangements of such cells with respect to each other allow the realization of various logical functions (NOT, AND, OR, *etc.*). Nomoto *et al.* [9] have studied a logic device AND/OR composed of a pair of tunnel-coupled quantum dots. They viewed unoccupation/occupation of a quantum dot by a single electron as a bit 0/1. Bandyopadhyay *et al.* [10] have discussed a concept of *spin gates*. In that approach the bits of information are carried by spins of individual electrons, e.g., the logical 1 (0) corresponds to the spin "up" ("down") direction of electron spin at a given quantum dot. In arrays of quantum dots, the quantum tunneling of electrons between adjacent dots and/or Coulomb interaction of electrons with each other play a role of "wiring", resulting in the signal propagation from dot to dot ('quantum coupled architecture').

Of course, the classical computational algorithms are not as efficient as the quantum ones since they do not benefit from purely quantum effects (superposition, interference, *etc.*). Nevertheless, one would expect that the reduction in size of computer components will result in increase of the computational speed (up to inverse atomic times) and data storage density (up to several units per nm² for planar structures). Besides, the Boolean logic seems to be more closer to a practical implementation at a nanometer scale. Indeed, a number of techniques have been developed to produce arrays of quantum dots on a solid surface (see, e.g., [10–12]). In addition, the scanning tunneling microscopy provides a direct way to write-in and read-out the information since the tunnel current is sensitive to the magnetic moment of a single atom [13]. Surely, the fabrication of classical logic devices based on quantum dots arrays will require more advanced technology. However it would be prudent to begin thinking now about the grounding in theory.

Let us discuss more closely the spin gates proposed by Bandyopadhyay *et al.* [10] and later investigated theoretically by Molotkov and Nazin [14] and by Krasheninnikov and Openov [15]. Such gates are assumed to consist of a number of tunnel-coupled quantum dots fabricated on a solid surface. The quantum dots play a role of potential wells for electrons. Each dot is supposed to have a single size-quantized energy level and there is, on the average, one electron per dot (the total number of electrons in the array of quantum dots can be controlled by adjusting the substrate voltage). In a spin gate, the stored information is determined by the spin configuration of the *ground state* of the

gate, i.e., by ground-state averages $\langle \hat{S}_{zi} \rangle$ of spin projection operators \hat{S}_{zi} at some dots (i is the number of a dot in the array).

Each spin gate has input and output dots. The input dots serve for writing the information to the gate through appropriate orientation of their electron spins (e.g., by the action of the local magnetic field generated by a magnetic STM tip). The external influence changes the Hamiltonian of the gate. The new ground state (and its spin configuration) is different from the initial one since there are electron interactions within (Coulomb repulsion) and between (tunneling and Coulomb repulsion) dots in the gate. The values of $\langle \hat{S}_{zi} \rangle$ at the output dots represent the result of calculations. The number of input and output dots in the gate depends on a particular logical function realized by the gate. For example, the AND gate has two inputs and one output, *etc.*

The "ground state computing" is the key idea for implementation of classical Boolean logic on a nanometer scale (we note that this idea was used not only for spin gates, but also for other kinds of quantum-dots-based gates, see, e.g., [8,9]). However, the concept of ground state computing has some essential drawbacks. The first one stems from the fact that the logical variables 1 and 0 are associated not with certain *pure* quantum states, but with some quantum-mechanical ground-state *averages*. For a particular case of spin gates, the logical 1 (0) at the dot i corresponds to a positive (negative) value of $\langle \hat{S}_{zi} \rangle$ or, more precisely, to $\langle \hat{S}_{zi} \rangle \geq S_t/2$ ($\langle \hat{S}_{zi} \rangle \leq -S_t/2$), where S_t is the "threshold value", $0 < S_t \leq 1$ [14,15]. We note, however, that in a complex quantum-mechanical system, the electron spin at any quantum dot is never directed strictly "up" or "down", so the value of S_t cannot be taken equal to unity. Theoretical analysis of several logical spin gates (NOT, AND, OR, NAND, NOR, XOR, NXOR, and half-adder) within the framework of spin-1/2 Heisenberg model has shown that for most of those gates the truth tables (which establish a one-to-one correspondence between the values of input and output bits) can be realized at sufficiently low values of S_t only ($S_t = 0.1$, or even $S_t = 0.05$ for half-adder) [14]. But the value of S_t should not be too low. Indeed, a low value of S_t does not imply that *average* projection of electron spin $\langle \hat{S}_{zi} \rangle$ at the dot i has low absolute value (so that it is hardly seen by a reading device). In fact, since an electron spin is a quantum-mechanical entity, we can detect only its "up" or "down" directions at any measurement. A low absolute value of $\langle \hat{S}_{zi} \rangle$ just means that a probability p_\uparrow to find an electron in the state with spin "up" doesn't differ much from a probability p_\downarrow to find an electron in the state with spin "down". But if so, we will not be able to draw a definite conclusion about the *sign* of $\langle \hat{S}_{zi} \rangle$ upon one particular measurement. In other words, there will be a high *error probability* P_{err} , i.e., by a definition, a high probability to measure $S_{zi} = -1/2$ while $\langle \hat{S}_{zi} \rangle > 0$, or to measure $S_{zi} = 1/2$ while $\langle \hat{S}_{zi} \rangle < 0$ ($P_{err} \approx 0.5$ if $S_t \ll 1$). This is detrimental for the computational efficiency.

For some simplest spin gates the issue of high error probability, related to low values of $|\langle \hat{S}_{zi} \rangle|$, can be resolved by applying a suitably directed uniform external magnetic field to the whole gate [15]. In particular, a fundamental possibility to reach ground-state averages $|\langle \hat{S}_{zi} \rangle| > 0.475$ at input and output dots of NOT-AND and NOT-OR three-dot spin gates has been demonstrated theoretically in [15]. Such a large value of $|\langle \hat{S}_{zi} \rangle|$ corresponds to $P_{err} < 0.05$. However, apart from the problem of low $|\langle \hat{S}_{zi} \rangle|$, the concept of ground state computing has one more serious limitation.

The point is that under the influence of external source on input dots of a spin gate, the relaxation of electronic subsystem to a new ground state can take place only through energy dissipation. The rate at which dissipation processes occur determines the speed of operation. However, whereas in two-dimensional nanostructures (quantum wells) the prevailing relaxation process is the emission of a longitudinal optical phonon with high relaxation rates of the order of 10^{12} s^{-1} , this process is forbidden in quantum dots because of the discrete nature of energy spectrum. Nomoto *et al.* [9] have shown that in semiconductor-based quantum dots, the emission of longitudinal acoustic phonon is the main contribution to the energy dissipation process. The relaxation rate is $(10^6 \div 10^9) \text{ s}^{-1}$, depending on geometrical parameters of an array of quantum dots [9]. The operation speed less than 10^9 s^{-1} is obviously too low for quantum-dots-based spin gates to be seriously considered as logic devices of new generation. Though some other scattering mechanisms (such as interface-phonon scattering) may also contribute to the energy dissipation in arrays of quantum dots [9], it is unlikely that they will cause the relaxation rate to increase significantly. Hence, it is reasonable to search for some other principles of spin gates operation, beyond the concept of ground state computing.

Recently Bandyopadhyay and Roychowdhury [16] have studied theoretically a possibility of *non-dissipative* operation of the simplest two-dot spin gate NOT (inverter). They showed that under the influence of local external magnetic field, the logical function can be realized at the stage of coherent temporal evolution of electronic subsystem in time less than 10^{-11} s , i.e., well before the relaxation to a new ground state takes place at the sacrifice of inelastic interactions. Moreover, it was shown [16] that there exists an optimal input signal energy to achieve a *complete switching* of the inverter, i.e., to realize spin configurations with saturated spin projections ($\langle \hat{S}_{zi} \rangle = 1/2$ or $-1/2$) at input and output dots. The results obtained in [16] are very encouraging. However, the authors of Ref. [16] used the spin-1/2 antiferromagnetic Heisenberg model to describe the correlated electrons in quantum dots constituting the inverter. As is known [17], the Heisenberg model is just a limiting case of the half-filled Hubbard model at $U \gg V$,

where U is the intra-dot Coulomb repulsion energy and V is the inter-dot tunneling energy. Since it is not clear *a priori* to what extent the Heisenberg model can describe the actual experimental situation, it is instructive to make use of more realistic Hubbard model, without any constraints on the ratio U/V .

In this paper we study the non-dissipative dynamics of the inverter within the framework of the Hubbard model (preliminary results have been presented in [18]). We explore a broad range of U and V values which physically correspond to various size of quantum dots and to various distance between them (the Heisenberg model as a limiting case at $U \gg V$ is also considered since it allows for a simple analytical solution). We show that complete switching of the inverter can be realized at unrealistic values of $U/V = 0$ and $U/V = \infty$ only. Nevertheless, it turns out that at *any* value of U/V one can reach averages $|\langle \hat{S}_{zi} \rangle| > 0.45$ at input and output dots in a very short operation time of the order of 10^{-11} s. Such large values of $|\langle \hat{S}_{zi} \rangle|$ correspond to the error probability $P_{err} < 0.1$ which is sufficiently low for implementation of logic function.

The paper is organized as follows. The Hubbard and Heisenberg models for the two-dot spin gate NOT (inverter) are described in Sec.2. The ground state computing is briefly outlined in Sec.3 for completeness sake. The temporal evolution of electronic subsystem, once the local external magnetic field is applied to the input dot, is studied in Sec.4, with special emphasis on time-dependent quantum-mechanical spin averages at input and output dots. We also analyze the dynamics of the inverter upon removing the input signal. The results obtained are discussed in Sec.5 from the viewpoint of prospects for non-dissipative computing in spin gates based on quantum dots. In Sec.6, concluding remarks are given.

2. Theoretical models

The inverter consists of two closely spaced quantum dots (A and B) occupied by two electrons [10,14,16]. One of two dots (say, the dot A) serves for writing the input signal to the gate by the action of the local external magnetic field H_A . The second dot (B) is the output.

A. Hubbard model

Under the assumption that each dot has only one size-quantized energy level, electron-dot interactions can be parametrized by one-electron Hartree-Fock on-site energies ϵ_A , ϵ_B , and the energy V of electron tunneling between the dots. Electron-electron interactions are specified by the energies U_{AA} , U_{BB} and U_{AB} of Coulomb repulsion between two electrons residing at the same dot or at different dots. We ignore the exchange Coulomb interaction between the dots [14] since, first, its characteristic energy is generally much smaller than U_{ij} ($i, j = A, B$) [19] and, second, the antiferromagnetic exchange naturally arises in the limiting case $V \ll U_{ij}$ which corresponds to the reduction of the Hubbard model to the Heisenberg one [17], see below. The presence of the (parallel to z -axis) local external magnetic field H_A at the dot A leads to the change in the total energy by μH_A , where μ is z -component of the magnetic moment at the dot A . In the site representation, the resulting Hubbard-like Hamiltonian has the form

$$\begin{aligned} \hat{H} = & \epsilon_A \sum_{\sigma} \hat{n}_{A\sigma} + \epsilon_B \sum_{\sigma} \hat{n}_{B\sigma} - V \sum_{\sigma} (\hat{a}_{A\sigma}^+ \hat{a}_{B\sigma} + \hat{a}_{B\sigma}^+ \hat{a}_{A\sigma}) + \\ & U_{AA} \hat{n}_{A\uparrow} \hat{n}_{A\downarrow} + U_{BB} \hat{n}_{B\uparrow} \hat{n}_{B\downarrow} + U_{AB} \sum_{\sigma, \sigma'} \hat{n}_{A\sigma} \hat{n}_{B\sigma'} - g\mu_B H_A \hat{S}_{zA}, \end{aligned} \quad (1)$$

where $\hat{a}_{i\sigma}$ ($\hat{a}_{i\sigma}^+$) are the operators for annihilation (creation) of electron with the spin projection $\sigma = \uparrow$ or \downarrow at the dot $i = A$ or B , $\hat{n}_{i\sigma} = \hat{a}_{i\sigma}^+ \hat{a}_{i\sigma}$ are the electron number operators, $\hat{S}_{zi} = (\hat{n}_{i\uparrow} - \hat{n}_{i\downarrow})/2$ is the operator of spin projection at the dot i , g is the Lande factor, μ_B is the Bohr magneton. The external magnetic field is directed along the magnetic moment of electron having $\sigma = \uparrow$.

Now let us slightly simplify the Hamiltonian (1), keeping all the key terms in it. First, we assume that the dots A and B are identical, so that $\epsilon_A = \epsilon_B = \epsilon_0$ and $U_{AA} = U_{BB} = U_0$. Second, we suppose that the total number of electrons in the inverter $N = \hat{n}_{A\uparrow} + \hat{n}_{A\downarrow} + \hat{n}_{B\uparrow} + \hat{n}_{B\downarrow}$ equals to 2 (one electron per dot, i.e., the half-filled band) and remains unchanged during the operation [14,16] at least till the reading of the result from the output dot. Then, by making use of the identity (see, e.g., [9])

$$2 \sum_{\sigma, \sigma'} \hat{n}_{A\sigma} \hat{n}_{B\sigma'} + 2\hat{n}_{A\uparrow} \hat{n}_{A\downarrow} + 2\hat{n}_{B\uparrow} \hat{n}_{B\downarrow} = N(N - 1),$$

we obtain

$$\hat{H} = -V \sum_{\sigma} (\hat{a}_{A\sigma}^+ \hat{a}_{B\sigma} + \hat{a}_{B\sigma}^+ \hat{a}_{A\sigma}) + (U_0 - U_{AB})(\hat{n}_{A\uparrow} \hat{n}_{A\downarrow} + \hat{n}_{B\uparrow} \hat{n}_{B\downarrow}) - \frac{g\mu_B H_A}{2} \sum_{\sigma} \hat{n}_{A\sigma} \text{sign}(\sigma) + \epsilon_0 N + U_{AB} \frac{N(N-1)}{2}, \quad (2)$$

where $\text{sign}(\sigma) = +1$ and -1 for $\sigma = \uparrow$ and \downarrow respectively. Finally, omitting two last non-operator terms from the Hamiltonian (2), we arrive at the expression

$$\hat{H} = -V \sum_{\sigma} (\hat{a}_{A\sigma}^+ \hat{a}_{B\sigma} + \hat{a}_{B\sigma}^+ \hat{a}_{A\sigma}) + U(\hat{n}_{A\uparrow} \hat{n}_{A\downarrow} + \hat{n}_{B\uparrow} \hat{n}_{B\downarrow}) - H \sum_{\sigma} \hat{n}_{A\sigma} \text{sign}(\sigma), \quad (3)$$

where we have introduced the renormalized energy of intra-dot Coulomb repulsion, $U = U_0 - U_{AB}$, and designated the input signal energy $H = g\mu_B H_A/2$. We note that generally $U > 0$ since $U_0 > U_{AB}$ [9].

The complete orthonormal set of inverter eigenstates is formed by the two-electron basis states

$$|1\rangle = |\uparrow, \downarrow\rangle, |2\rangle = |\downarrow, \uparrow\rangle, |3\rangle = |\uparrow\downarrow, 0\rangle, |4\rangle = |0, \uparrow\downarrow\rangle, |5\rangle = |\uparrow, \uparrow\rangle, |6\rangle = |\downarrow, \downarrow\rangle, \quad (4)$$

where, e.g., the notation $|\uparrow, \downarrow\rangle$ denotes the state with up-spin electron at the dot A and down-spin electron at the dot B , the notation $|\uparrow\downarrow, 0\rangle$ denotes the state with two (up-spin and down-spin) electrons at the dot A and no electrons at the dot B , *etc.* We stress that the spin projection on either of the two quantum dots is zero in the basis states $|3\rangle$ and $|4\rangle$. In this respect the NOT gate based on two *quantum dots* differs in general from the "spatially extended NOT gate" based on two *spins* [20]. In fact, the latter corresponds to the limiting case $U \gg V$ of the Hamiltonian (3) and may be described within the framework of the Heisenberg model, see below.

In the virgin state (i.e., at $H = 0$), the time-dependent electron wave function $\Psi_0(t)$ is the solution of the Schrödinger equation

$$i\hbar \partial \Psi_0(t) / \partial t = \hat{H} \Psi_0(t) \quad (5)$$

with the Hamiltonian (3) taken at $H = 0$ and can be represented as

$$\Psi_0(t) = \sum_{k=1}^6 A_k^{(0)} \Psi_k^{(0)} \exp(-iE_k^{(0)} t / \hbar), \quad (6)$$

where the coefficients $A_k^{(0)}$ do not depend on time, and $\Psi_k^{(0)}$ and $E_k^{(0)}$ ($k = 1 \div 6$) are eigenvectors and eigenenergies of the stationary Schrödinger equation

$$\hat{H} \Psi_k^{(0)} = E_k^{(0)} \Psi_k^{(0)} \quad (7)$$

They are as follows:

$$\begin{aligned} \Psi_1^{(0)} &= \frac{1}{\sqrt{2}}(|1\rangle - |2\rangle), \quad \Psi_2^{(0)} = \frac{1}{\sqrt{2}}(|3\rangle - |4\rangle), \\ \Psi_3^{(0)} &= \frac{1}{2} \sqrt{1 + \frac{U}{\sqrt{U^2 + 16V^2}}} \left(|1\rangle + |2\rangle + \frac{\sqrt{U^2 + 16V^2} - U}{4V} |3\rangle + \frac{\sqrt{U^2 + 16V^2} - U}{4V} |4\rangle \right), \\ \Psi_4^{(0)} &= \frac{1}{2} \sqrt{1 - \frac{U}{\sqrt{U^2 + 16V^2}}} \left(|1\rangle + |2\rangle - \frac{\sqrt{U^2 + 16V^2} + U}{4V} |3\rangle - \frac{\sqrt{U^2 + 16V^2} + U}{4V} |4\rangle \right), \\ \Psi_5^{(0)} &= |5\rangle, \quad \Psi_6^{(0)} = |6\rangle, \end{aligned} \quad (8)$$

and

$$E_1^{(0)} = 0, \quad E_2^{(0)} = U, \quad E_3^{(0)} = -\frac{\sqrt{U^2 + 16V^2} - U}{2}, \quad E_4^{(0)} = \frac{\sqrt{U^2 + 16V^2} + U}{2}, \quad E_5^{(0)} = 0, \quad E_6^{(0)} = 0. \quad (9)$$

Generally, the coefficients $A_k^{(0)}$ in (6) can take any values which satisfy the normalization condition

$$\sum_{k=1}^6 |A_k^{(0)}|^2 = 1. \quad (10)$$

In other words, the electronic subsystem can exist in a rather complex superposition of quantum eigenstates $\Psi_k^{(0)}$.

In the presence of the input signal at the dot A , the time-dependent wave function $\Psi(t)$ satisfies the Schrödinger equation (5) with the Hamiltonian (3), and can be expanded as

$$\Psi(t) = \sum_{k=1}^6 A_k \Psi_k \exp(-iE_k t/\hbar), \quad (11)$$

where Ψ_k and E_k ($k = 1 - 6$) are eigenvectors and eigenenergies of the stationary Schrödinger equation

$$\hat{H}\Psi_k = E_k \Psi_k, \quad (12)$$

and the time-independent coefficients A_k satisfy the normalization condition

$$\sum_{k=1}^6 |A_k|^2 = 1. \quad (13)$$

At arbitrary values of U , V , and H the eigenvalue equation (12) reduces to the algebraic equation of the third power in E_k . The resulting expressions are too cumbersome for analysis, so it is more convenient to solve the equation (12) numerically. However, it is useful for the following discussion to consider a special case $U = 0$ which physically corresponds to $U \ll V$ (closely-spaced large-sized dots [9]). At $U = 0$ and at arbitrary values of V and H we have for eigenvectors and eigenenergies of the equation (12) rather simple analytical expressions:

$$\begin{aligned} \Psi_1 &= \sqrt{\frac{2V^2}{H^2 + 4V^2}} \left(|1\rangle - |2\rangle - \frac{H}{2V}|3\rangle - \frac{H}{2V}|4\rangle \right), \quad \Psi_2 = \frac{1}{\sqrt{2}}(|3\rangle - |4\rangle), \\ \Psi_3 &= \frac{\sqrt{H^2 + 4V^2} + H}{2\sqrt{H^2 + 4V^2}} \left(|1\rangle + \frac{\sqrt{H^2 + 4V^2} - H}{\sqrt{H^2 + 4V^2} + H}|2\rangle + \frac{\sqrt{H^2 + 4V^2} - H}{2V}|3\rangle + \frac{\sqrt{H^2 + 4V^2} - H}{2V}|4\rangle \right), \\ \Psi_4 &= \frac{\sqrt{H^2 + 4V^2} - H}{2\sqrt{H^2 + 4V^2}} \left(|1\rangle + \frac{\sqrt{H^2 + 4V^2} + H}{\sqrt{H^2 + 4V^2} - H}|2\rangle - \frac{\sqrt{H^2 + 4V^2} + H}{2V}|3\rangle - \frac{\sqrt{H^2 + 4V^2} + H}{2V}|4\rangle \right), \\ \Psi_5 &= |5\rangle, \quad \Psi_6 = |6\rangle, \end{aligned} \quad (14)$$

and

$$E_1 = 0, \quad E_2 = 0, \quad E_3 = -\sqrt{H^2 + 4V^2}, \quad E_4 = \sqrt{H^2 + 4V^2}, \quad E_5 = -H, \quad E_6 = H. \quad (15)$$

One can see that expressions (14) and (15) taken at $H = 0$ coincide with expressions (8) and (9) taken at $U = 0$ respectively.

B. Heisenberg model

In the limiting case $U \gg V$ (widely-spaced small-sized dots [9]), the half-filled Hubbard model reduces to the spin-1/2 antiferromagnetic Heisenberg model [17]. The corresponding Hamiltonian for the inverter has the form [14,16]:

$$\hat{H} = J \sum_{\alpha} \hat{\sigma}_{\alpha A} \hat{\sigma}_{\alpha B} - H \sum_{\sigma} \hat{n}_{A\sigma} \text{sign}(\sigma), \quad (16)$$

where $\hat{\sigma}_{\alpha i}$ ($\alpha = x, y, z$) are the Pauli matrices describing the electron at the dot $i = A$ or B and $J = V^2/U$ is the energy of exchange interaction between two electrons residing at dots A and B . We have omitted the term $-J(\hat{n}_{A\uparrow} + \hat{n}_{A\downarrow})(\hat{n}_{B\uparrow} + \hat{n}_{B\downarrow})$ [17] from (16) since in the Heisenberg model the complete orthonormal set of inverter eigenstates doesn't include the two-electron states $|3\rangle = |\uparrow\downarrow, 0\rangle$ and $|4\rangle = |0, \uparrow\downarrow\rangle$, see (4), so that each dot is occupied by one electron, and hence $(\hat{n}_{A\uparrow} + \hat{n}_{A\downarrow})(\hat{n}_{B\uparrow} + \hat{n}_{B\downarrow}) = 1$ is just a c -number.

The Heisenberg model for the inverter allows for analytical solution at any values of J and H [14,16] (in what follows we shall make use of this fact to analyze the case $U \gg V$). The eigenvectors and eigenenergies of the stationary Schrödinger equation with the Hamiltonian (16) are as follows:

$$\begin{aligned}
\Psi_1 &= \sqrt{\frac{1}{2} \left(1 + \frac{H}{\sqrt{H^2 + 4J^2}}\right)} |1\rangle - \sqrt{\frac{1}{2} \left(1 - \frac{H}{\sqrt{H^2 + 4J^2}}\right)} |2\rangle, \\
\Psi_2 &= \sqrt{\frac{1}{2} \left(1 - \frac{H}{\sqrt{H^2 + 4J^2}}\right)} |1\rangle + \sqrt{\frac{1}{2} \left(1 + \frac{H}{\sqrt{H^2 + 4J^2}}\right)} |2\rangle, \\
\Psi_3 &= |5\rangle, \quad \Psi_4 = |6\rangle,
\end{aligned} \tag{17}$$

and

$$E_1 = -J - \sqrt{H^2 + 4J^2}, \quad E_2 = -J + \sqrt{H^2 + 4J^2}, \quad E_3 = J - H, \quad E_4 = J + H. \tag{18}$$

The time-dependent wave function $\Psi(t)$ has the form (11) with Ψ_k and E_k given by (17) and (18) respectively except that the number of inverter eigenstates in the Heisenberg model is less by two than in the Hubbard one, so that the summation over k in (11) is from $k = 1$ up to $k = 4$.

3. Ground state computing

The truth table of the logical gate NOT is very simple, the output bit B being just the inverse of the input bit A , i.e., $B = \bar{A}$ ($B = 1$ if $A = 0$ and $B = 0$ if $A = 1$). Let us see how this truth table is realized if the input and output bits are encoded in *ground state* averages $\langle \hat{S}_{zA} \rangle$ and $\langle \hat{S}_{zB} \rangle$ respectively. We shall ascribe the bit 1 (0) at the dot i to the positive (negative) value of $\langle \hat{S}_{zi} \rangle$, with the constraint $|\langle \hat{S}_{zi} \rangle| \geq S_t/2$, where $0 < S_t \leq 1$ [14,15].

As discussed in the Introduction, one wishes to have S_t as large as possible since the greater is S_t , the lower is the error probability P_{err} , i.e., the probability to read the "wrong" signal S_{zi} at the dot i (e.g., to measure $S_{zi} = -1/2$ while $\langle \hat{S}_{zi} \rangle > 0$). The physical reason for a possibility of such an error in the device operation is the entangled structure of the ground state wave function (the latter cannot be factored as $|\uparrow\rangle_A |\downarrow\rangle_B$ or $|\downarrow\rangle_A |\uparrow\rangle_B$). It is straightforward to find the upper limit of P_{err} as a function of S_t . For the sake of definiteness, let us consider the case $\langle \hat{S}_{zA} \rangle \geq S_t/2$, $\langle \hat{S}_{zB} \rangle \leq -S_t/2$ which corresponds to $H > 0$. Then $P_{err} = 1 - p_{\uparrow\downarrow}$ where $p_{\uparrow\downarrow}$ is the quantum-mechanical probability to find up-spin electron at the dot A and down-spin electron at the dot B . Since, by a definition, $\langle \hat{S}_{zA} \rangle = (p_{\uparrow\downarrow} - p_{\downarrow\uparrow})/2$, one has generally $p_{\uparrow\downarrow} - p_{\downarrow\uparrow} \geq S_t$, and hence $P_{err} \leq 1 - S_t$ (in the special case $U \gg V$, the ground state eigenvector is composed of states $|\uparrow, \downarrow\rangle$ and $|\downarrow, \uparrow\rangle$ only, see (4), (17), (18), and one has $p_{\uparrow\downarrow} + p_{\downarrow\uparrow} = 1$, $p_{\uparrow\downarrow} \geq (1 + S_t)/2$, and $P_{err} \leq (1 - S_t)/2$). Note that $P_{err} = 0$ in the ideal case $S_t = 1$ only, i.e., in the case of saturated spin projections $|\langle \hat{S}_{zi} \rangle| = 1/2$ at both dots $i = A$ and B .

It follows from (8) and (9) that at zero input signal $H = 0$ the ground state of the inverter at any value of the ratio U/V is the entangled state $\Psi_3^{(0)}$ with zero magnetic moments at both dots A and B since $\langle \Psi_3^{(0)} | \hat{S}_{zA} | \Psi_3^{(0)} \rangle = \langle \Psi_3^{(0)} | \hat{S}_{zB} | \Psi_3^{(0)} \rangle = 0$. At $H \neq 0$, the ground state averages of spin projections at the input and output dots become nonzero. They are equal in magnitude and opposite in sign, $\langle \hat{S}_{zA} \rangle = -\langle \hat{S}_{zB} \rangle$, just as required by the truth table of the inverter. Making use of (14) and (15), one has

$$\langle \hat{S}_{zA} \rangle = \frac{H}{2\sqrt{H^2 + 4V^2}}, \quad U \ll V, \tag{19}$$

while

$$\langle \hat{S}_{zA} \rangle = \frac{H}{2\sqrt{H^2 + 4J^2}}, \quad U \gg V \tag{20}$$

as follows from (17) and (18). At arbitrary value of the ratio U/V , the dependence of $\langle \hat{S}_{zA} \rangle$ on H may be approximated as $\langle \hat{S}_{zA} \rangle = H/2\sqrt{H^2 + 4W^2}$ where $W = Vf(U/V)$, and the function $f(x)$ is shown in Fig. 1 ($f(0) = 1$; $f(x) = 1/x$ at $x \gg 1$). Thus, $\langle \hat{S}_{zA} \rangle$ increases monotonically with H from $\langle \hat{S}_{zA} \rangle = 0$ at $H = 0$ and asymptotically approaches its maximum value $\langle \hat{S}_{zA} \rangle = 1/2$ at $H \gg W$. The error probability is close to 0.75 (for $U \ll V$) or 0.5 (for $U \gg V$) at $H \ll W$ and decreases with H as $P_{err} \approx \alpha W^2/H^2$ at $H \gg W$ ($\alpha = 2$ and 1 for $U \ll V$ and $U \gg V$ respectively).

In order to minimize P_{err} one should have the input signal energy as high as possible. However this cannot be easily realized experimentally since realistic values of $H_A \leq 1$ T correspond to quite low values of $H \leq 0.1$ meV, while H should be much greater than the characteristic energy W . On the other hand, the energy W should exceed considerably the thermal energy $k_B T$ for stable operation [16], so the operating temperature should be restricted to at least 100 mK.

Aside from the problem of P_{err} reduction, the speed of device operation is limited by the finite rate of relaxation of electronic subsystem to a new ground state upon applying the input signal (see the Introduction). The relaxation rate is determined by dissipation processes, so the dissipation is a necessary attribute of the ground state computing in the array of quantum dots. In what follows we study a possibility to perform a logical operation NOT *in the absence of dissipation*, at the stage of non-dissipative temporal evolution of electronic subsystem.

4. Non-dissipative computing

Our purpose is to calculate the quantum-mechanical averages

$$S_{zA}(t) = -S_{zB}(t) = \langle \Psi(t) | \hat{S}_{zA} | \Psi(t) \rangle \quad (21)$$

at $t \geq 0$, i.e., upon applying the input signal to the dot A . For definiteness, we shall consider the case $H_A > 0$ (i.e., $H > 0$). We shall also assume that at $t \leq 0$ (in the absence of external signal) the system is in its ground state, so that the time-dependent wave function at $t \leq 0$ is $\Psi_0(t) = \Psi_3^{(0)} \exp(-iE_3^{(0)}t/\hbar)$, see (8), (9), and hence the coefficients $A_k^{(0)}$ in the expansion of $\Psi_0(t)$ (6) have the values $A_1^{(0)} = A_2^{(0)} = A_4^{(0)} = A_5^{(0)} = A_6^{(0)} = 0$, $A_3^{(0)} = 1$.

The coefficients A_k in the expansion of the time-dependent wave function $\Psi(t)$ (11) at $t \geq 0$ should be found from the initial condition $\Psi(t=0) = \Psi_0(t=0)$. It is convenient to write the eigenvectors Ψ_k of the stationary Schrödinger equation (12) as

$$\Psi_k = \sum_{n=1}^6 B_{kn} |n\rangle. \quad (22)$$

Then

$$\Psi(t) = \sum_{n=1}^6 f_n(t) |n\rangle, \quad (23)$$

where

$$f_n(t) = \sum_{k=1}^6 A_k B_{kn} \exp(-iE_k t/\hbar). \quad (24)$$

The probability to find the system in the basis state $|n\rangle$ at time t is

$$p_n(t) = |f_n(t)|^2. \quad (25)$$

Since, as follows from (4), $\langle 1 | \hat{S}_{zA} | 1 \rangle = 1/2$, $\langle 2 | \hat{S}_{zA} | 2 \rangle = -1/2$, $\langle 3 | \hat{S}_{zA} | 3 \rangle = \langle 4 | \hat{S}_{zA} | 4 \rangle = 0$, $\langle 5 | \hat{S}_{zA} | 5 \rangle = 1/2$, $\langle 6 | \hat{S}_{zA} | 6 \rangle = -1/2$, one has from (21), (23), (25):

$$S_{zA}(t) = -S_{zB}(t) = \frac{p_1(t) - p_2(t) + p_5(t) - p_6(t)}{2}. \quad (26)$$

First we consider the limiting case $U \ll V$ [18] (the weak coupling limit of the Hubbard model). Setting $U = 0$, we have rather simple equations for the probabilities $p_n(t)$:

$$\begin{aligned} p_1(t) &= \frac{1}{4} \left(1 + \frac{4HV}{H^2 + 4V^2} \sin^2(\omega t/2) \right)^2, \\ p_2(t) &= \frac{1}{4} \left(1 - \frac{4HV}{H^2 + 4V^2} \sin^2(\omega t/2) \right)^2, \\ p_3(t) &= p_4(t) = \frac{1}{4} \left(1 - \frac{16H^2V^2}{(H^2 + 4V^2)^2} \sin^4(\omega t/2) \right), \\ p_5(t) &= p_6(t) = 0, \end{aligned} \quad (27)$$

where

$$\omega = \sqrt{H^2 + 4V^2}/\hbar. \quad (28)$$

From (26) and (27) it is straightforward to find that

$$S_{zA}(t) = -S_{zB}(t) = \frac{2HV}{H^2 + 4V^2} \sin^2(\omega t/2). \quad (29)$$

It follows from (29) that at any positive values of H and V the function $S_{zA}(t)$ is non-negative and oscillates in time with the frequency ω (given by (28)) and the amplitude

$$S_{zA}(t_0) = \frac{2HV}{H^2 + 4V^2}, \quad (30)$$

where t_0 stands for the time of the first peak of $S_{zA}(t)$,

$$t_0 = \frac{\pi}{\omega} = \frac{\pi\hbar}{\sqrt{H^2 + 4V^2}}. \quad (31)$$

The curve $S_{zA}(t)$ is shown in Fig. 2 for several different values of H/V . From Fig. 2 and (28), (31) one can see that the oscillation frequency ω monotonically increases (i.e., the time t_0 decreases) with H , while the amplitude $S_{zA}(t_0)$ first increases with H , reaches the maximum value $1/2$ at $H = 2V$ and then decreases, being in inverse proportion to H at $H \gg V$. Thus, a *complete* switching, $S_{zA}(t_0) = 1/2$ and $S_{zB}(t_0) = -1/2$, is achieved at $H/V = 2$ and $t_0 = \pi\hbar/2\sqrt{2}V$.

It should be stressed that though the function $S_{zA}(t)$, being periodic in time, has its peak value at $t_k = \pi/\omega + 2\pi k/\omega$ (k is an integer), here and below we are interested in the *lowest* possible value of t_k (i.e., t_0) since we want not only to reach the maximum permissible value of S_{zA} , but to do it in as short as possible switching time.

Now let us turn to the opposite limiting case, $U \gg V$ (the strong coupling limit of the Hubbard model). This case may be described within the framework of the Heisenberg model (16). It has been considered by Bandyopadhyay and Roychowdhury in [16]. For the sake of completeness, we briefly sketch the results obtained in [16].

As we have noted above, in the Heisenberg model, the complete set of inverter eigenstates doesn't include the states $|3\rangle = |\uparrow\downarrow, 0\rangle$ and $|4\rangle = |0, \uparrow\downarrow\rangle$, see (4), (17). For the probabilities $p_n(t)$ to find the system in the basis states $|n\rangle = |1\rangle, |2\rangle, |5\rangle$ and $|6\rangle$ one has

$$\begin{aligned} p_1(t) &= \frac{1}{2} \left(1 + \frac{4HJ}{H^2 + 4J^2} \sin^2(\omega t/2) \right), \\ p_2(t) &= \frac{1}{2} \left(1 - \frac{4HJ}{H^2 + 4J^2} \sin^2(\omega t/2) \right), \\ p_5(t) &= p_6(t) = 0, \end{aligned} \quad (32)$$

where

$$\omega = 2\sqrt{H^2 + 4J^2}/\hbar \quad (33)$$

(we recall that $J = V^2/U \ll V$ is the energy of antiferromagnetic exchange). From (26) and (32) one has

$$S_{zA}(t) = -S_{zB}(t) = \frac{2HJ}{H^2 + 4J^2} \sin^2(\omega t/2). \quad (34)$$

One can see from (34) that the function $S_{zA}(t)$ at $U \gg V$ has the same form as in the case $U \ll V$ (29). The difference between the two cases is that V in (28) and (29) is replaced by J in (33) and (34) respectively, and that there is an extra factor of 2 in the oscillation frequency in (33) as compared with (28). The amplitude of the function $S_{zA}(t)$ is

$$S_{zA}(t_0) = \frac{2HJ}{H^2 + 4J^2}, \quad (35)$$

where t_0 is the time of the first peak of $S_{zA}(t)$,

$$t_0 = \frac{\pi}{\omega} = \frac{\pi\hbar}{2\sqrt{H^2 + 4J^2}}. \quad (36)$$

It follows from (35) and (36) that a *complete* switching, $S_{zA}(t_0) = 1/2$ and $S_{zB}(t_0) = -1/2$, is achieved at $H/J = 2$ and $t_0 = \pi\hbar/4\sqrt{2}J$.

Thus, having considered two limiting cases of weak ($U \ll V$) and strong ($U \gg V$) electron coupling, we see that the complete switching of the inverter can take place in either limit of the Hubbard model providing a proper choice of the values of the input signal energy H and the switching time t_0 . Hence, one may expect that the complete switching can occur also in the case of intermediate coupling, at an arbitrary ratio of U to V (i.e., at arbitrary values of the size of quantum dots and the distance between them).

To check this hypothesis, we have calculated numerically the dependencies of S_{zA} on t at different values of U/V and H/V . Several typical examples of S_{zA} versus t curves are shown in Fig. 3. The switching time t_0 was generally defined as a time of the first peak on the curve $S_{zA}(t)$, t_0 being a function of U/V and H/V . As opposed to the cases of weak and strong coupling considered above, at arbitrary values of U/V and H/V the function $S_{zA}(t)$ is not periodic in time since it includes several harmonics with different frequencies and amplitudes. Hence, in principle, the value of $S_{zA}(t)$ greater than $S_{zA}(t_0)$ can be achieved at some longer time (see, e.g., Fig. 3b). But this case is of no interest for us since our purpose is not only to maximize S_{zA} , but also to minimize the switching time.

The curves of $S_{zA}(t_0)$ versus H/V are shown in Fig. 4 for several values of U/V . One can see that an increase in U/V first results in a decreased height of the maximum S_{zA}^{max} on the $S_{zA}(t_0)$ versus H/V curve. For $U/V > 2$ the value of S_{zA}^{max} increases once more, but doesn't reach the saturation value $1/2$ at finite U/V , though $S_{zA}^{max} \rightarrow 1/2$ if $U/V \rightarrow \infty$ (this corresponds to the Heisenberg model and agrees with the results obtained in [16]). Fig. 5 shows the dependence of S_{zA}^{max} on U/V . Note that $S_{zA}^{max} \geq 0.45$ at any U/V .

We define H_{opt} as the "optimal" value of input signal energy H , i.e., as the value of H at which the peak value $S_{zA}(t_0)$ reaches its maximum S_{zA}^{max} at a given U/V (e.g., $H_{opt} = 2V$ at $U/V = 0$, see (30); $H_{opt} = 2J = 2V^2/U$ at $U \gg V$, see (35); $H_{opt} = 0.83V$ at $U/V = 2$, see Fig. 4). The dependence of H_{opt}/V on U/V is plotted in Fig. 6. One can see from this figure that H_{opt}/V decreases monotonically with increasing U/V . It is remarkable that the equation $H_{opt}/V = 2V/U$ derived analytically in the Heisenberg model, i.e., for $U \gg V$ (35), is a good approximation of the numerically calculated curve even at $U \approx V$. It follows from Fig. 6 that the curves $S_{zA}(t)$ shown in Figs. 3a and 3b are for the case $H > H_{opt}$ while the curve $S_{zA}(t)$ shown in Fig. 3c is for the case $H = H_{opt}$ (hence, the peak value of $S_{zA}(t_0)$ in Fig. 3c is the maximum permissible value of $S_{zA}(t)$ at $U/V = 1.5$).

An important characteristic of the logical gate is its switching time t_0 which depends on U/V and H/V (see above). At a given U/V , we define the "optimal" switching time t_{opt} as the time of the first peak on the curve $S_{zA}(t)$ at $H = H_{opt}$. Hence, $S_{zA}(t_{opt})$ equals to S_{zA}^{max} , the maximum permissible value of $S_{zA}(t_0)$ at fixed U/V (see Fig. 4). The dependence of t_{opt} on U/V is shown in Fig. 7. It is seen that t_{opt} increases monotonically with increasing U/V from $t_{opt} = \pi\hbar/2\sqrt{2}V$ at $U/V = 0$, see (31), and approaches the curve $t_{opt} = \pi\hbar U/4\sqrt{2}V^2$, derived analytically in the Heisenberg model, for $U \gg V$, see (36).

It is instructive to examine the dynamics of the inverter upon removing the external signal from the input dot A at a time $t = T$ without reading the spin polarization in the output dot B . At $t > T$ the electronic subsystem continues to evolve in accordance with the Schrödinger equation (5). For the sake of simplicity, we restrict our consideration to the case $U \gg V$ (Heisenberg model) since this allows for a simple analytical solution. For the quantum-mechanically averaged spin projections at the dots A and B we have

$$S_{zA}(t) = -S_{zB}(t) = S_0 \sin \left(\frac{4J(t-T)}{\hbar} + \arctan \left(\frac{2J}{\sqrt{H^2 + 4J^2}} \tan(\omega T/2) \right) \right), \quad (37)$$

where

$$S_0 = \frac{H}{H^2 + 4J^2} \sqrt{(H^2 \cos^2(\omega T/2) + 4J^2) \sin^2(\omega T/2)} \quad (38)$$

and ω is given by Eq. (33). We see that $S_{zA}(t)$ and $S_{zB}(t)$ oscillate between $-S_0$ and S_0 having zero average values. The amplitude of oscillations S_0 depends not only on the values of H and J but on the value of T as well. If $H \geq 2J$ then S_0 has its maximum value $1/2$ at $\omega T = \arccos(-4J^2/H^2) + 2\pi k$ where k is an integer. It is interesting that $S_0 = 0$ at $\omega T = 2\pi k$, i.e., $S_{zA}(t) = -S_{zB}(t) \equiv 0$, just as in the ground state at $H = 0$. In this case the result of two subsequent perturbations at $t = 0$ and $t = T$ is such that the system at $t > T$ behaves as if it was not perturbed at all. This effect can be explained in a way that the two perturbations interfere in a counterphase thus compensating each other.

5. Discussion

In Sec. 3 we saw that in the presence of input signal at the dot A the *ground state* average of the spin projection $\langle \hat{S}_{zA} \rangle$ increases monotonically with increasing the input signal energy H from $\langle \hat{S}_{zA} \rangle = 0$ at $H = 0$ and asymptotically

approaches the saturation value $\langle \hat{S}_{zA} \rangle = 1/2$ at $H \gg W$ where $W = Vf(U/V)$ is a characteristic energy which depends on U and V ($W = V$ at $U/V = 0$ and $W = J = V^2/U$ at $U/V \gg 1$, see Fig. 1). In the case of temporal evolution of electronic subsystem upon application of the input signal to the dot A one would expect the peak value $S_{zA}(t_0)$ of the time-dependent spin projection $S_{zA}(t) = \langle \Psi(t) | \hat{S}_{zA} | \Psi(t) \rangle$ be also governed by the same parameter, the ratio H/W . As follows from analytical expressions (30) and (35) obtained for $S_{zA}(t_0)$ in the limiting cases $U/V \ll 1$ and $U/V \gg 1$ respectively, this is so indeed. However, unlike the ground state average $\langle \hat{S}_{zA} \rangle$, the dependence of $S_{zA}(t_0)$ on H/W is *nonmonotonic*. By contrast, $S_{zA}(t_0)$ has a maximum S_{zA}^{max} at a *finite* value of H/W while tending to zero at $H/W \gg 1$, see (30), (35), Fig. 4, and Fig. 6. Hence there is a fundamental difference between the physical processes responsible for an increase of the spin projection in the static and dynamic cases.

We stress that perfect antiferromagnetic spin ordering with maximum absolute values of spin projections on both dots, $S_{zA} = -S_{zB} = 1/2$, can be realized at the stage of coherent temporal evolution not only in the limit $U/V \rightarrow \infty$ (this would seem natural by analogy with the static case when large values of U/V are favorable for antiferromagnetism [17]) but also in the limit $U/V \rightarrow 0$. This effect, which we have called "dynamical antiferromagnetism", arises from the peculiar nature of electronic transitions under the influence of external perturbation.

So, in the case of temporal non-dissipative evolution of the inverter, the maximum permissible (for given U and V) value of S_{zA} is achieved at a *finite* value of the input signal energy H , i.e., $S_{zA} = S_{zA}^{max}$ at $H = H_{opt}$ and $t = t_{opt}$, see Figs. 2 - 4. It is important that $S_{zA}^{max} \geq 0.45$ at any ratio U/V while $S_{zA}^{max} \rightarrow 1/2$ at $U/V \rightarrow 0$ or $V/U \rightarrow 0$, see Fig. 5. Since $S_{zB}(t) = -S_{zA}(t)$ at any time, then if the spin polarization (logical bit) at the output dot B is measured at a time $t = t_{opt}$, the inversed input signal, i.e., $S_{zB} = -1/2$ for $H > 0$ or $S_{zB} = 1/2$ for $H < 0$, is detected with high probability. In other words, the error probability P_{err} , i.e., the probability to measure the wrong output signal ($S_{zB} = 1/2$ for $H > 0$ or $S_{zB} = -1/2$ for $H < 0$) is very low. Indeed, the upper limit of P_{err} may be estimated as $P_{err}(t) \leq 1 - 2S_{zA}(t)$, see Sec. 3. At $t = t_{opt}$ one has $P_{err}(t_{opt}) \leq 1 - 2S_{zA}^{max}$, i.e., $P_{err}(t_{opt}) \ll 1$ at $U \ll V$ or $U \gg V$, the maximum value of $P_{err}(t_{opt})$ being about 0.1 at $U/V = 2$.

We recall (see Sec. 3) that in order to reduce P_{err} in ground state computing, one should increase the input signal energy H . In the case of interest, $P_{err} \ll 1$, it can be shown from (19) and (20) that $H \approx W/\sqrt{P_{err}}$, where W is a characteristic energy that determines the scale of the energy levels scheme of the inverter, see Fig. 1. But if so, the value of H should be also much greater than the thermal energy $k_B T$ since the inequality $k_B T \ll W$ must be fulfilled in order the inverter was in its ground state. Thus, in fact, one should have

$$k_B T \ll W \ll H \quad (39)$$

in ground state computing. This condition is obviously hardly realizable since even the temperature as low as $T = 1$ K corresponds to rather high magnetic field about 1 T, and hence at $T = 1$ K two strong inequalities in (39) can be satisfied only for unrealistic magnetic field about 100 T. Otherwise the error probability P_{err} is very high.

In the case of non-dissipative computing, there is no need for the relaxation to the new ground state since the perfect antiferromagnetic ordering of magnetic moments is realized at the stage of unitary evolution when an appropriate superposition of the inverter eigenstates takes place, see above. Hence, the input signal energy H should not be anomalously high. For example, in the limiting case $U \gg V$, the optimal value of H is $H_{opt} = 2V^2/U$, so that, e.g., at $V \approx 1$ meV and $U \approx 10$ meV the external magnetic field acting on the input dot can be relatively low, about 1 T. Such a magnetic field is generated, e.g., by the magnetic moment of the order of μ_B in its vicinity. Hence, the input signal may be thought of as being supplied by the output quantum dot of another gate whose magnetic moment has been oriented in such way or another at the previous stage of calculations.

We note that the limiting case $U \gg V$ is much more suitable for the physical implementation than the case $U \ll V$. Indeed, at $U \ll V$ we have $H_{opt} = 2V$, hence for a realistic value of the input magnetic field about 1 T, the Coulomb repulsion energy U should not exceed 0.01 meV in order to satisfy the inequality $U \ll V$. Since $U \approx e^2/\epsilon a$, where a is the dot size and ϵ is the dielectric constant [21], for $U \approx 0.01$ meV one has $a \approx 10^4 - 10^5$ nm. Such a relatively large structure obviously can not be considered as a quantum *dot*.

Though the switching of the inverter to the new ground state upon the influence of the external signal is not necessary in non-dissipative computing, we stress that our results on unitary evolution of electronic subsystem of the inverter are obtained under the assumption that at $t \leq 0$ (in the absence of the external signal) the inverter is in its *ground state*. Thus, one faces the problem of preparing such an initial state of the inverter, and consequently, the problem of temperature reduction, as in the case of ground state computing. In this respect, it would be interesting to search for such a type of input signal (e.g., for such a direction of the external magnetic field, see [20]) whose influence on the input dot will result in the desired temporal evolution of electronic subsystem (and consequently, in the realization of the truth table) irrespective of the initial state of the inverter.

The other facing problem is the reading of the result of computation (output). While in ground state computing the output can be read at *any* moment after relaxation of the system to its new ground state, in non-dissipative

computing the reading time must be chosen with a great accuracy as a time when spin projections at the dots have their maximal values, in order to minimize the error probability. It is interesting to analyze the relationship between the "optimal" values of t_{opt} and H_{opt} . The dependence of the product $t_{opt}H_{opt}$ on U/V is shown in Fig. 8. One can see that the value of $t_{opt}H_{opt}$ decreases monotonically with U/V from $\pi\hbar/\sqrt{2}$ at $U/V = 0$, see (30), (31) down to $\pi\hbar/2\sqrt{2}$ at $U/V \rightarrow \infty$, see (35), (36). Thus, the relationship

$$t_{opt} \approx \hbar/H_{opt} \quad (40)$$

holds true for the whole range of U/V . In general, this is a consequence of the Heisenberg's uncertainty principle.

We recall that our purpose is to minimize the switching time t_{opt} and thereby to maximize the speed of computation. But according to (40), the decrease in t_{opt} can be achieved only at the sacrifice of increase in H_{opt} . Since the value of the input signal energy is finite, the relationship (40) imposes a restriction on t_{opt} . For realistic value of external magnetic field ≈ 1 T one has $t_{opt} \approx 10^{-11}$ s.

6. Conclusions

The system consisting of two tunnel-coupled quantum dots, input and output ones, occupied by two electrons has been considered within the framework of the Hubbard model with arbitrary values of the parameters, the intra-dot Coulomb energy U and the inter-dot tunneling energy V . After applying the external signal (the local magnetic field) to the input dot, the magnetic moments of the dots become oriented in opposite directions, i.e., align antiferromagnetically. This allows one to use such a system as the quantum spin gate "inverter" realizing the truth table of logical NOT.

In ground state computing, the inverter switches (relaxes) to the new ground state under the influence of the input signal. Since the relaxation process is due to inelastic interactions, the switching time is of the order of $10^{-9} \div 10^{-6}$ s which is rather long on the atomic scale. Moreover, the magnetic moments of the dots are far from being saturated, giving rise to the large probability of reading the wrong result of computation from the output dot. For these reasons the principle of ground state computing seems to be ineffective for the spin logical gates.

We have suggested a new approach which overcomes the two above mentioned drawbacks of ground state computing. Our approach takes advantage of the coherent non-dissipative evolution of electronic subsystem after applying the signal to the input dot at $t = 0$. We have demonstrated that at *any* moment $t > 0$ magnetic moments of the dots arrange in antiferromagnetic order, i.e., $S_{zA}(t) = -S_{zB}(t)$, thus realizing the truth table of the inverter. The value of $S_{zA}(t)$ (and hence $S_{zB}(t)$ as well) is a nonmonotonic function of time, being a periodic function in the limiting cases $U \ll V$ and $U \gg V$. At given values of V , U , and the input signal energy H there always exists a moment t_0 which corresponds to the first local maximum on the curve $S_{zA}(t)$. Besides, there exists an "optimal" value H_{opt} at which the magnitude of $S_{zA}(t_0)$ reaches its maximum permissible (for a given ratio of U/V) value S_{zA}^{max} , thus reducing the error probability P_{err} . Our calculations showed that $S_{zA}^{max} \geq 0.45$ at any U and V , being close to $1/2$ at $U \ll V$ and $U \gg V$. So, the value of $P_{err} \ll 1$ is well below than that in ground state computing. The "optimal" values of H_{opt} and $t_{opt} = t_0(H_{opt})$ are related by Eq. (40). For reasonable values of U , V and realistic magnetic fields ~ 1 T one has $t_{opt} \approx 10^{-11}$ s, several orders of magnitude less than in ground state computing.

Note that the effect of "dynamical antiferromagnetism" appears to be usable for further development of more complicated spin gates consisting of a greater number of quantum dots. However, several problems should be resolved. First, our results are obtained for a particular case that the initial state of the inverter is its *ground* state. It would be desirable to search for such a type of the input signal (e.g., for such an orientation of the external magnetic field with respect to the quantization axis) that the complete switching of the inverter took place irrespective of its initial state (the latter may be a superposition of inverter eigenstates). Second, there is a problem of reading of the result of computation. If the direction of the magnetic moment on the output dot is measured at a time different from the "optimal" time t_{opt} , then the error probability increases. We note that the quantum-mechanical average of the spin projection at the output dot of the inverter has the same sign at any time after the input signal had been applied to the input dot (this sign determines the value of the logical bit at the output). Hence, should the electron spin be a classical vector, then the result of calculation could be determined unambiguously. It would be very interesting to search for such a measurement procedure that enabled us to draw a conclusion about the *average* direction of the magnetic moment over some period of time. Solving of these problems appears to be the target of future research.

Acknowledgments

This work was supported in part by the Russian Foundation for Fundamental Research under Grant No 96-02-18918 and by the Russian State Program "Advanced Technologies and Devices in Micro- and Nanoelectronics" under Grant

No 02.04.329.89.5.3. We are grateful to S.Bandyopadhyay for sending us a preprint of the work [16] prior to publication and to I.A.Semenihin for the help at the early stage of this work. We would like to thank A.V.Krasheninnikov, S.N.Molotkov, and S.S.Nazin for fruitful discussions.

- [1] R.Feynman, Intern. J. Theor. Phys., 21 (1982) 467.
- [2] C.H.Bennett, Physics Today, October (1995) 24, and references therein.
- [3] P.Shor, Proc. of the 35th Annual Symposium on the Foundations of Computer Science, IEEE Computer Society Press, Los Alamitos, CA, (1994) 124.
- [4] Q.A.Turchette, C.J.Hood, W.Lange, H.Mabuchi, H.J.Kimble, Phys. Rev. Lett., 75 (1995) 4710.
- [5] C.Monroe, D.M.Meekhof, B.E.King, W.M.Itano, D.J.Wineland, Phys. Rev. Lett., 75 (1995) 4714.
- [6] S.Haroche, J.-M.Raimond, Physics Today, August (1996) 51.
- [7] R.Landauer, Phys. Lett. A, 217 (1996) 188.
- [8] C.S.Lent, P.D.Tougaw, J. Appl. Phys., 74 (1993) 6227; C.S.Lent, P.D.Tougaw, W.Porod, G.H.Bernstein, Nanotechnology, 4 (1993) 49.
- [9] K.Nomoto, R.Ugajin, T.Suzuki, I.Hase, J. Appl. Phys., 79 (1996) 291.
- [10] S.Bandyopadhyay, B.Das, A.E.Miller, Nanotechnology, 5 (1994) 113; S.Bandyopadhyay, V.P.Roychowdhury, X.Wang, Phys. Low-Dim. Struct., 8/9 (1995) 28.
- [11] H.J.Mamin, P.H.Guethner, D.Rugar, Phys. Rev. Lett., 65 (1990) 2418.
- [12] B.Meurer, D.Heitmann, K.Ploog, Phys. Rev. Lett., 68 (1992) 1371.
- [13] R.Wiesendanger, H.-J.Güntherodt, G.Güntherodt, R.J.Cambino, R.Ruf, Phys. Rev. Lett., 65 (1990) 583.
- [14] S.N.Molotkov, S.S.Nazin, Pis'ma v ZhETF, 62 (1995) 256 [JETP Lett., 62 (1995) 273]; ZhETF, 110 (1996) 1439 [JETP, 83 (1996) 794].
- [15] A.V.Krasheninnikov, L.A.Openov, Pis'ma v ZhETF, 64 (1996) 214 [JETP Lett., 64 (1996) 231].
- [16] S.Bandyopadhyay, V.P.Roychowdhury, Superlattices and Microstructures, to be published.
- [17] Yu.A.Izyumov, Uspekhi Fiz. Nauk, 161 (1991) 1 [Sov. Phys. Usp., 34 (1991) 935]; Uspekhi Fiz. Nauk, 165 (1995) 403 [Phys. Usp., 38 (1995) 385]; Uspekhi Fiz. Nauk, 167 (1997) 465 [Phys. Usp., 40 (1997) 455].
- [18] A.M.Bychkov, L.A.Openov, I.A.Semenihin, Pis'ma v ZhETF, 66 (1997) 275 [JETP Lett., 66 (1997) 298].
- [19] J.Hubbard, Proc. Roy. Soc. A, 276 (1963) 238.
- [20] D.Mozyrsky, V.Privman, S.P.Hotaling, Int. J. Mod. Phys. B, 11 (1997) 2207.
- [21] A.V.Krasheninnikov, S.N.Molotkov, S.S.Nazin, L.A.Openov, ZhETF, 112 (1997) 1257 [JETP, 85 (1997) 682].

Figure captions

Fig.1. The function $f(x)$ entering into the expression for the ground state average of the spin projection $\langle \hat{S}_{zA} \rangle = H/2\sqrt{H^2 + 4V^2}f^2(U/V)$ at the quantum dot A .

Fig.2. Temporal evolution of the quantum-mechanically averaged spin projection $S_{zA}(t) = \langle \Psi(t) | \hat{S}_{zA} | \Psi(t) \rangle$ at the quantum dot A upon applying the local external magnetic field H_A to the dot A . The intradot Coulomb repulsion energy $U = 0$ at both dots A and B (the weak coupling limit of the Hubbard model). $H = V$ (dashed line), $H = 2V$ (solid line), $H = 6V$ (dotted line). Here $H = g\mu_B H_A/2$ is the input signal energy, V is the energy of electron tunneling between the quantum dots, the time t is measured in units of \hbar/V .

Fig.3. The same as in Fig.2, for a) $U/V = 2$, $H/V = 2$; b) $U/V = 1$, $H/V = 4$; c) $U/V = 1.5$, $H/V = 1.155$.

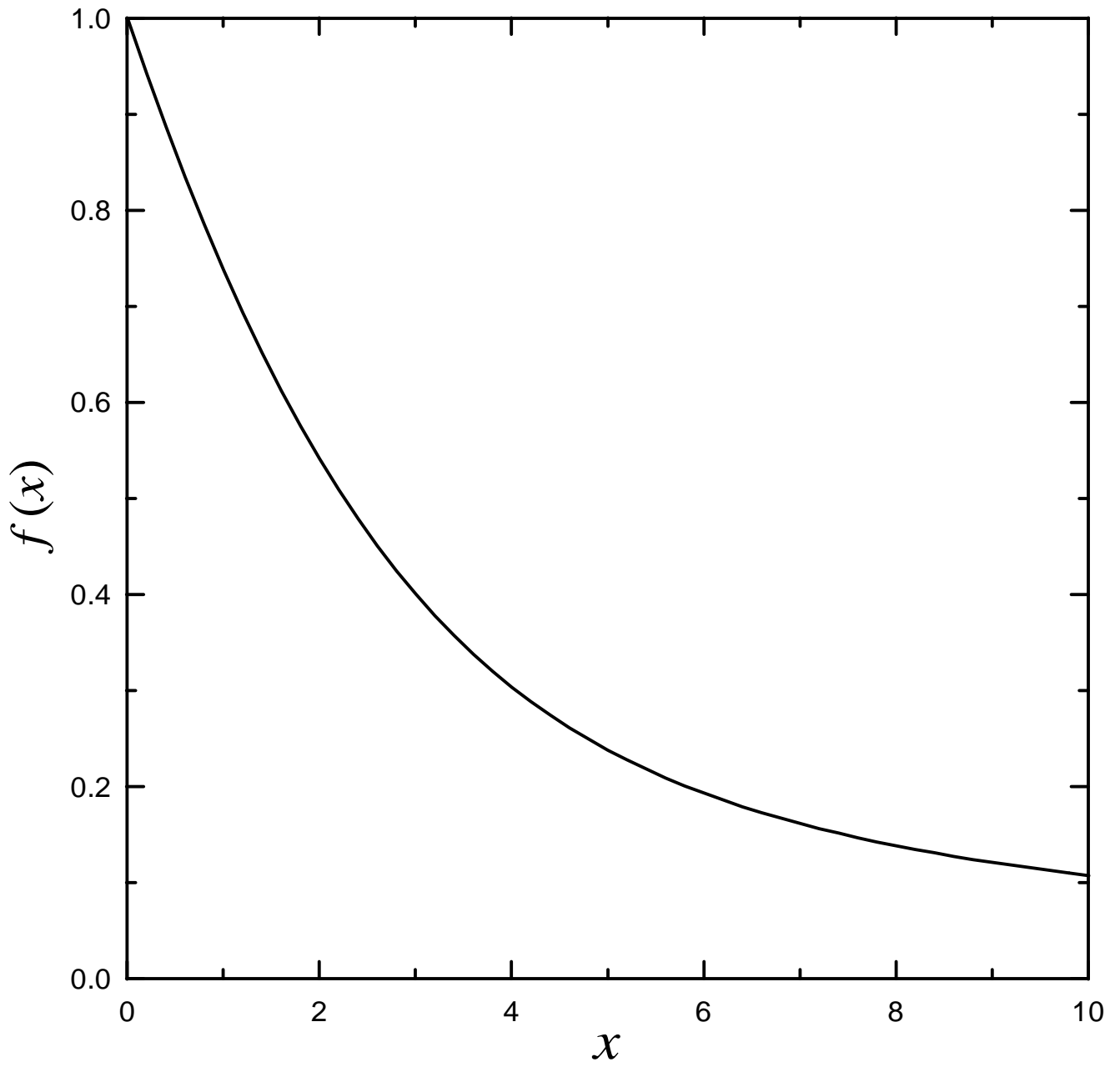
Fig.4. The peak value of $S_{zA}(t_0)$ versus H/V at different U/V . The switching time t_0 is defined as a time of the first peak at the curve $S_{zA}(t)$ at given values of U/V and H/V .

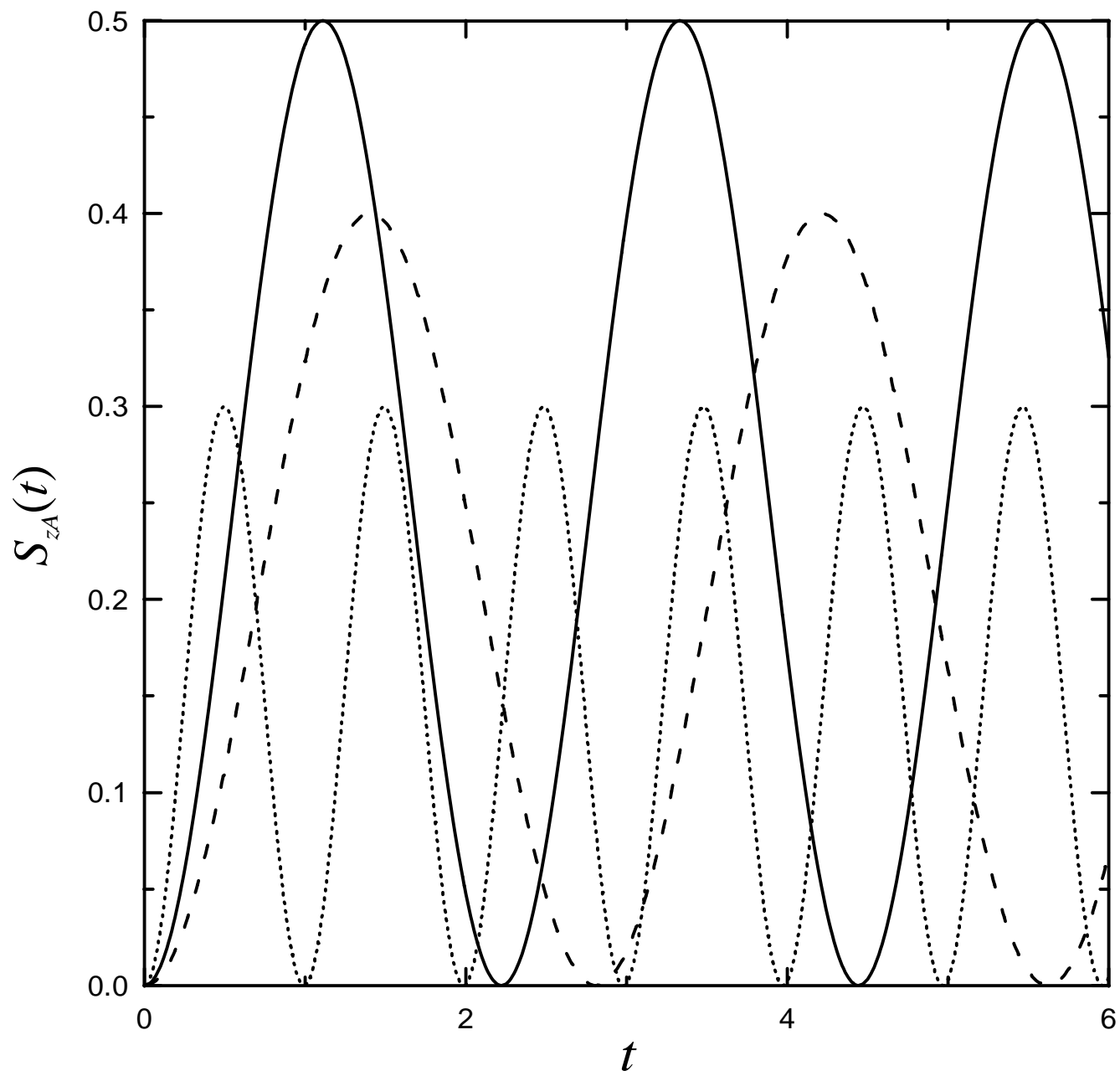
Fig.5. The dependence of S_{zA}^{max} on U/V . Here S_{zA}^{max} is the maximum value of $S_{zA}(t_0)$ on the $S_{zA}(t_0)$ versus H/V curve at a given U/V .

Fig.6. The "optimal" value of normalized input signal energy H_{opt}/V versus U/V . Here H_{opt} is the value of H at which the peak value $S_{zA}(t_0)$ reaches its maximum S_{zA}^{max} at a given U/V , see Fig.4. Solid line is the result of numerical calculations. Dashed line is the curve $H_{opt}/V = 2V/U$ obtained in the Heisenberg model, i.e., for $U \gg V$.

Fig.7. The "optimal" switching time t_{opt} measured in units of \hbar/V as a function of U/V . Here t_{opt} is the time of the first peak on the curve $S_{zA}(t)$ at $H = H_{opt}$, i.e., $t_{opt}(U/V) = t_0(U/V, H_{opt}/V)$ corresponds to S_{zA}^{max} , the maximum permissible value of $S_{zA}(t_0)$ at a given U/V . Solid line is the result of numerical calculations. Dashed line is the curve $t_{opt}V/\hbar = \pi U/4\sqrt{2}V$ obtained in the Heisenberg model, i.e., for $U \gg V$.

Fig.8. The product of "optimal" switching time t_{opt} measured in units of \hbar/V by the "optimal" value of normalized input signal energy H_{opt}/V versus U/V .





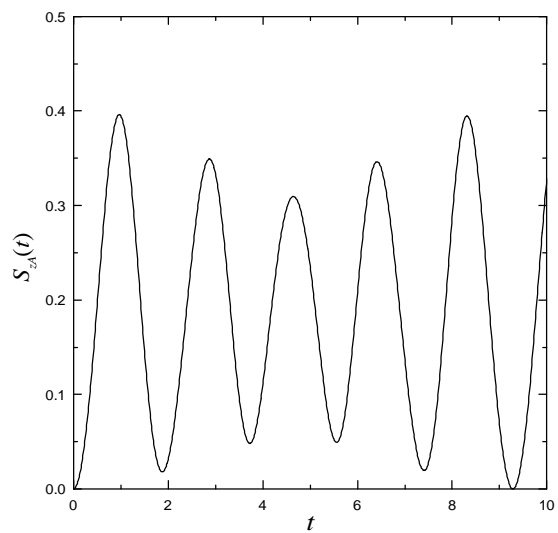


Figure 3a

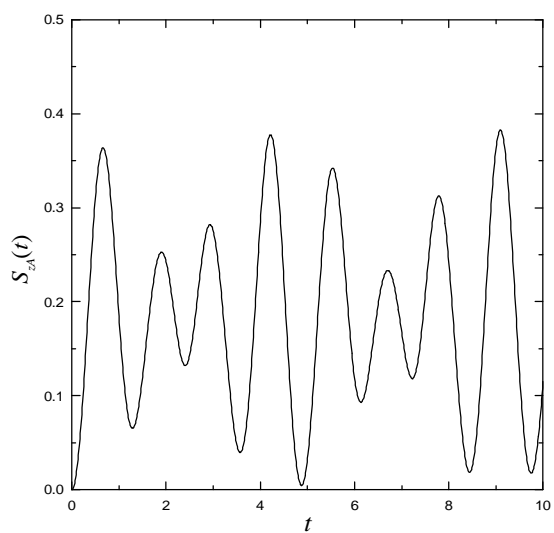


Figure 3b

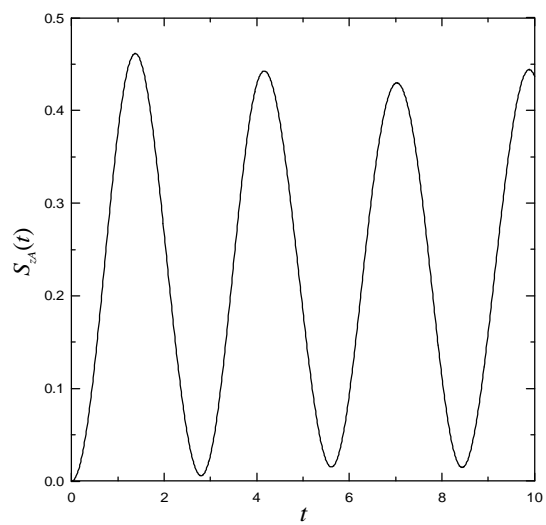


Figure 3c

